SIMULATION OF LOCALIZED SURFACE PLASMON RESONANCES IN TWO DIMENSIONS VIA IMPEDANCE–IMPEDANCE OPERATORS *

DAVID P. NICHOLLS † AND XIN TONG†

Abstract. It is critically important that engineers be able to numerically simulate the scattering of electromagnetic radiation by bounded obstacles. Additionally, that these simulations be robust and highly accurate is necessitated by many applications of great interest. High–Order Spectral algorithms applied to interfacial formulations can rapidly deliver high fidelity approximations with a modest number of degrees of freedom. The class of High–Order Perturbation of Surfaces methods have proven to be particularly appropriate for these simulations and in this contribution we consider questions of both practical implementation and rigorous analysis. For the former we generalize our recent results to utilize the uniformly well–defined Impedance–Impedance Operators rather than the Dirichlet–Neumann Operators which occasionally encounter unphysical singularities. For the latter we utilize this new formulation to establish the existence, uniqueness, and analyticity of solutions in non–resonant configurations. We also include results of numerical simulations based on an implementation of our new formulation which demonstrates its noteworthy accuracy and robustness.

Key words. High–Order Spectral Methods, Linear Wave Scattering, Bounded Obstacles, High–Order Perturbation of Surfaces Methods

AMS subject classifications. 65N35, 65N12, 78A45, 78M22, 35Q60, 35J05

1. Introduction.

It is critically important that engineers be able to numerically simulate the scattering of electromagnetic radiation by bounded obstacles. Applications abound, and solely in the field of plasmonics [38, 23] one find surface enhanced Raman scattering (SERS) biosensing [43], imaging [22], and cancer therapy [10]. For more details please see one of the many surveys on the topic, e.g., the volume [23] (Chapters 5, 9, and 10), the article [25], and the publications considering gold nanoparticles [26]. For many reasons, these simulations must be robust and highly accurate, e.g., due to the very strong plasmonic effect (the field enhancement can be several orders of magnitude) and its quite sensitive nature (the enhancement is only seen over a range of tens of nanometers in incident radiation for gold and silver particles).

As in our previous contribution [37], we focus on Localized Surface Plasmon Resonances (LSPRs) which can be induced in metal (e.g., gold or silver) nanorods with radiation in the visible range. In particular how these change as the shape of the cross–section of the rod is varied from perfectly circular. More specifically, consider a rod with cross–section shaped by $\{r = \bar{g}\}$, composed of a noble metal with a wavelength–dependent permittivity, $\epsilon_m = \epsilon_m(\lambda) \in \mathbf{C}$, mounted in a dielectric with constant permittivity, $\epsilon_d \in \mathbf{R}$. If $\bar{g}$ is sufficiently small an LSPR is excited with incident radiation of wavelength, λ_F, that (nearly) satisfies the two–dimensional "Fröhlich condition" [23]

$$\mathrm{Re}\,[\epsilon_m(\lambda)] = -\epsilon_d. \tag{1.1}$$

It is clear, however, that if the cross–section of the rod is specified by $r = \bar{g} + \varepsilon f(\theta)$, where $\bar{g}$ is the mean radius, for some smooth function f, then the value $\lambda_F = \lambda_F(\varepsilon)$ will change. The method we advocate here is well–suited to study the evolution in ε.

*D.P.N. gratefully acknowledges support from the National Science Foundation through grant No. DMS–1813033.

†Department of Mathematics, Statistics, and Computer Science, University of Illinois at Chicago, Chicago, IL 60607 (davidn@uic.edu,xtong20@uic.edu)

Due to the importance of these models, it is not surprising that the full range of modern numerical methods have been brought to bear upon this problem, including Finite Difference Methods [21], Finite Element Methods [18], Discontinous Galerkin Methods [17], Spectral Element Methods [9], and Spectral Methods [13]. We have recently argued [37] that such *volumetric* approaches are greatly disadvantaged with an unnecessarily large number of unknowns for the piecewise homogeneous problems of relevance here. Interfacial methods based upon Integral Equations (IEs) [6] deliver a compelling class of algorithms (see, e.g., the recent work of [1, 16] in the context of plasmonics) but, as we have pointed out, these also face difficulties. Most of these have been addressed in recent years through the use of sophisticated quadrature rules to deliver High–Order Spectral accuracy, and the design of preconditioned iterative solvers with suitable acceleration [14]. Consequently, they specify a method which deserves serious consideration (see, e.g., the recent work of [20]), however, two properties render them non–competitive for the *parameterized* problems we consider compared to the methods we outline here:

1. We parameterize our geometry by the real value ε (the deviation of the nanorod cross–section from circular), and an IE solver will compute the scattering data only for one value of ε at a time. If this value is changed then the solver must be run again.
2. The dense, non–symmetric positive definite systems of linear equations which must be inverted with each simulation.

As we have previously shown [37], a "High–Order Perturbation of Surfaces" (HOPS) approach can mollify these concerns. In particular, we investigated an implementation of the method of Field Expansions (FE) originating in the low–order calculations of Rayleigh [39] and Rice [40]. The high–order implementation was developed by Bruno & Reitich [4] and later enhanced and stabilized by the first author and Reitich [34], the first author and Nigam [29], and the first author and Shen [35], resulting in the Method of Transformed Field Expansions (TFE). We point out that with this latter approach these methods can be shown to be convergent for *real* ε of *arbitrarily* large size, up to topological obstruction [33, 34]. These algorithms retain the advantageous properties of classical IE methods (e.g., surface formulation and exact enforcement of far–field conditions) while avoiding the shortcomings listed above:

1. Since HOPS algorithms are built upon expansions in the parameter, ε, once the Taylor coefficients are known for the scattering quantities, it is simply a matter of summing these (rather than beginning a new simulation) for any given choice of ε to recover the returns.
2. At every Taylor order, the method need only invert a single, sparse operator corresponding to the cylindrical–interface, order–zero approximation of the problem.

In this contribution we build upon the work of the authors in [37] by devising, implementing, and testing a HOPS scheme based not upon Dirichlet–Neumann Operators (DNOs), but rather upon Impedance–Impedance Operators (IIOs). We do this for several reasons, principally that our new approach does not suffer from the artificial "Dirichlet eigenvalues" which plague the relevant DNOs while requiring no increase in computational effort. In addition, we supply for the first time a rigorous analysis of the existence, uniqueness, and analyticity of solutions to the problem of scattering of linear waves by a penetrable object of bounded cross–section (see also the work of Bonnet–Ben Dhia, Carvalho, Chesnel, and Ciarlet [3] who investigated a related problem with a non–perturbative technique). While the technique of proof is well–established [31, 33, 34, 28] the technical details are rather involved, c.f. [15, 7, 30], and somewhat limited by the complication of *rigorously* establishing that physical configurations are "non–resonant." Finally, with an implementation of this algorithm we display the efficiency, robustness, and high–order accuracy one can achieve.

The paper is organized as follows: In § 2 we outline the governing equations for linear waves reflected and transmitted by a cylindrical obstacle, with transparent boundary conditions described in § 2.1. We give a boundary formulation of the resulting problem in § 3, together with a HOPS algorithm in § 3.1 and a study of the classical problem of scattering by a rod in § 3.2. For use with our rigorous analysis we define our function spaces in § 4, and we deliver our proof of analyticity of solutions in § 5. The fundamental results required in the proof are the analyticity of the IIOs proven in § 6. Finally, in § 7 we present numerical results followed by concluding remarks in § 8.

2. Governing Equations.

We consider a y–invariant obstacle of bounded cross–section as displayed in Figure 1. Materials of refractive index $n^u \in \mathbf{R}$ and $n^w \in \mathbf{C}$ fill the (unbounded) exterior and (bounded) interior, respectively. The interface between the two domains is described in polar coordinates, $\{x = r\cos(\theta), z = r\sin(\theta)\}$, by the graph $r = \bar{g} + g(\theta)$ so that the exterior and interior domains are specified by $S^u := \{r > \bar{g} + g(\theta)\}$, $S^w := \{r < \bar{g} + g(\theta)\}$, respectively. The superscripts are chosen to conform to the notation of previous work by the authors [27, 37]. The cylindrical geometry demands that the interface be 2π–periodic, $g(\theta + 2\pi) = g(\theta)$. We

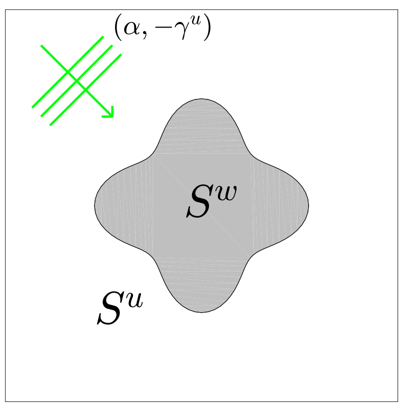

FIG. 1. *Plot of the cross–section of a nanorod (occupying S^w) shaped by $r = \bar{g} + \varepsilon\cos(4\theta)$ ($\varepsilon = \bar{g}/5$) housed in a dielectric (occupying S^u) under plane–wave illumination with wavenumber $(\alpha, -\gamma^u)$.*

consider monochromatic plane–wave illumination by incident radiation of frequency ω and wavenumber $k^u = n^u\omega/c_0 = \omega/c^u$ (c_0 is the speed of light) aligned with the corrugations of the obstacle. We denote the reduced illuminating fields of incidence angle ϕ

$$\mathbf{E}^{\text{inc}} = \mathbf{A}e^{i\alpha x - i\gamma^u z}, \quad \mathbf{H}^{\text{inc}}(x,z) = \mathbf{B}e^{i\alpha x - i\gamma^u z},$$
$$\alpha = k^u\sin(\phi), \quad \gamma^u = k^u\cos(\phi), \quad |\mathbf{A}| = |\mathbf{B}| = 1;$$

we have factored out time dependence of the form $\exp(-i\omega t)$, and we can write these as $\mathbf{E}^{\text{inc}} = \mathbf{A}e^{ik^u r\sin(\phi-\theta)}$, $\mathbf{H}^{\text{inc}} = \mathbf{B}e^{ik^u r\sin(\phi-\theta)}$. The geometry demands that the reduced electric and magnetic fields, $\{\mathbf{E}, \mathbf{H}\}$, be 2π–periodic in θ, and the scattered radiation is "outgoing" in S^u and bounded in S^w.

In this two–dimensional setting the time–harmonic Maxwell equations decouple into two scalar Helmholtz problems which govern the transverse electric (TE) and transverse magnetic (TM) polarizations [38]. The invariant (y) directions of the scattered (electric or magnetic) fields are denoted by $\{u(r,\theta), w(r,\theta)\}$ in S^u and S^w, respectively, and the incident radiation in the outer domain by $u^{\text{inc}}(r,\theta)$.

These developments lead us to seek outgoing/bounded, 2π–periodic solutions of

$$\Delta u + (k^u)^2 u = 0, \qquad r > \bar{g} + g(\theta), \tag{2.1a}$$

$$\Delta w + (k^w)^2 w = 0, \qquad r < \bar{g} + g(\theta), \tag{2.1b}$$

$$u - w = \xi, \qquad r = \bar{g} + g(\theta), \tag{2.1c}$$

$$\tau^u \partial_N u - \tau^w \partial_N w = \tau^u \nu, \qquad r = \bar{g} + g(\theta), \tag{2.1d}$$

where $k^w = n^w \omega / c_0$, the Dirichlet data is

$$\xi(\theta) := \left[-u^{\text{inc}}\right]_{r=\bar{g}+g(\theta)} = -e^{ik^u(\bar{g}+g(\theta))\sin(\phi-\theta)}, \tag{2.1e}$$

and the Neumann data is

$$\begin{aligned}\nu(\theta) &:= \left[-\partial_N u^{\text{inc}}\right]_{r=\bar{g}+g(\theta)} \\ &= \left\{(\bar{g}+g(\theta)) i k^u \sin(\phi-\theta) + \left(\frac{g'(\theta)}{\bar{g}+g(\theta)}\right)\cos(\phi-\theta)\right\}\xi(\theta).\end{aligned}$$

In these $\partial_N = \hat{r}(\bar{g}+g)\partial_r - \hat{\theta}(g'/(\bar{g}+g))\partial_\theta$, for unit vectors in the radial ($\hat{r}$) and angular ($\hat{\theta}$) directions, and

$$\tau^m = \begin{cases} 1, & \text{TE}, \\ 1/\epsilon^{(m)}, & \text{TM}, \end{cases} \qquad m \in \{u, w\},$$

where $\gamma^w = k^w \cos(\phi)$. The case of TM polarization is of fundamental importance in the study of Localized Surface Plasmon Resonances (LSPRs) [38] and thus we concentrate our attention on the TM case from here.

2.1. Transparent Boundary Conditions. Regarding the outgoing nature of u we demand the Sommerfeld Radiation Condition [6], and to enforce both this and the boundedness of w, we introduce the circles $\{r = R^{(u)}\}$ and $\{r = R^{(w)}\}$, where

$$R^{(u)} > \bar{g} + |g|_{L^\infty}, \quad 0 < R^{(w)} < \bar{g} - |g|_{L^\infty}.$$

We note that we can find periodic solutions of the relevant Helmholtz problems on the domains $\{r > R^{(u)}\}$ and $\{r < R^{(w)}\}$, respectively, given generic Dirichlet data, say $\underline{u}(\theta)$ and $\underline{w}(\theta)$. These read [6]

$$u(r,\theta) = \sum_{p=-\infty}^{\infty} \hat{\underline{u}}_p \frac{H_p(k^u r)}{H_p(k^u R^{(u)})} e^{ip\theta}, \quad w(r,\theta) = \sum_{p=-\infty}^{\infty} \hat{\underline{w}}_p \frac{J_p(k^w r)}{J_p(k^w R^{(w)})} e^{ip\theta}, \tag{2.2}$$

where J_p is the p–th Bessel function of the first kind, and H_p is the p–th Hankel function of the first kind. We note that

$$u(R^{(u)},\theta) = \sum_{p=-\infty}^{\infty} \hat{\underline{u}}_p e^{ip\theta}, \quad w(R^{(w)},\theta) = \sum_{p=-\infty}^{\infty} \hat{\underline{w}}_p e^{ip\theta}.$$

With these formulas we can compute the *outward–pointing* Neumann data at the artificial boundaries

$$-\partial_r u(R^{(u)},\theta) = \sum_{p=-\infty}^{\infty} \left(-k^u \frac{H_p'(k^u R^{(u)})}{H_p(k^u R^{(u)})} \right) \hat{\underline{u}}_p e^{ip\theta} =: T^{(u)} \left[\underline{u}(\theta) \right],$$

$$\partial_r w(R^{(w)},\theta) = \sum_{p=-\infty}^{\infty} \left(k^w \frac{J_p'(k^w R^{(w)})}{J_p(k^w R^{(w)})} \right) \hat{\underline{w}}_p e^{ip\theta} =: T^{(w)} \left[\underline{w}(\theta) \right].$$

These define the order–one Fourier multipliers $\{T^{(u)}, T^{(w)}\}$.

With the operator $T^{(u)}$ it is not difficult to see that periodic, outward propagating solutions to the Helmholtz equation

$$\Delta u + (k^u)^2 u = 0, \quad r > \bar{g} + g(\theta),$$

equivalently solve

$$\Delta u + (k^u)^2 u = 0, \qquad \bar{g} + g(\theta) < r < R^{(u)}, \tag{2.3a}$$

$$\partial_r u + T^{(u)} [u] = 0, \qquad r = R^{(u)}. \tag{2.3b}$$

Similarly, one can show that periodic, bounded solutions to the Helmholtz equation

$$\Delta w + (k^w)^2 w = 0, \quad r < \bar{g} + g(\theta),$$

equivalently solve

$$\Delta w + (k^w)^2 w = 0, \qquad R^{(w)} < r < \bar{g} + g(\theta),$$

$$\partial_r w - T^{(w)} [w] = 0, \qquad r = R^{(w)}.$$

3. Boundary Formulation. At this point we follow the philosophy of [27, 28, 37] and reduce our degrees of freedom to surface unknowns. However, rather than select the Dirichlet and Neumann traces utilized in these papers, we choose impedance traces. To motivate our particular choices we focus upon the boundary conditions (2.1c) and (2.1d) and operate upon this pair by the linear operator

$$P = \begin{pmatrix} Y & -I \\ Z & -I \end{pmatrix},$$

where I is the identity, and Y and Z are unequal operators to be specified. In the work of Despres [8] these were chosen to be $\mp i\eta$ for a constant $\eta \in \mathbf{R}^+$, however, other choices are also possible. The resulting boundary conditions are

$$[-\tau^u \partial_N u + Y u] + [\tau^w \partial_N w - Y w] = [-\tau^u \nu + Y \xi],$$

$$[-\tau^u \partial_N u + Z u] + [\tau^w \partial_N w - Z w] = [-\tau^u \nu + Z \xi],$$

which inspire the following definitions for impedances

$$U := [-\tau^u \partial_N u + Y u]_{r=\bar{g}+g}, \quad W := [\tau^w \partial_N w - Z w]_{r=\bar{g}+g},$$

their "conjugates"

$$\tilde{U} := [-\tau^u \partial_N u + Z u]_{r=\bar{g}+g}, \quad \tilde{W} := [\tau^w \partial_N w - Y w]_{r=\bar{g}+g},$$

and the interfacial data

$$\zeta := \left[-\tau^u \nu + Y \xi \right], \quad \psi := \left[-\tau^u \nu + Z \xi \right].$$

Via an integral formula these quantities can deliver the scattered field at *any* point [11, 6], thus, the governing equations reduce to the boundary conditions

$$U + \tilde{W} = \zeta, \quad \tilde{U} + W = \psi. \tag{3.1}$$

Now, we have two equations for four unknowns, however, the pairs $\{U, \tilde{U}\}$ and $\{W, \tilde{W}\}$ are not independent and we make this explicit through the introduction of Impedance–Impedance operators (IIOs). However, care is required as a poor choice of the operators Y or Z may induce a lack of uniqueness in the governing Helmholtz equation, i.e., $(k^u)^2$ or $(k^w)^2$ may be an eigenvalue of the Laplacian (with the impedance boundary conditions) on the domain in question.

As our analysis utilizes a change of variables which transforms the general interface shape, $\{r = \bar{g} + g(\theta)\}$, to the separable one, $\{r = \bar{g}\}$, our developments focus on solving Helmholtz problems on the interior of the cylinder $\{r < \bar{g}\}$ and its exterior $\{r > \bar{g}\}$. For this reason, in Appendix A we state and briefly prove two results on the existence, uniqueness, and regularity of solutions to the exterior and interior Helmholtz problems on these simple domains. For now we note that in order to have well–defined solutions (and thus IIOs) we demand the following two conditions

$$\operatorname{Im} \left\{ \int_\Gamma \left(\left(\frac{Y}{\tau^u} \right) u \right) \overline{u} \, ds \right\} \leq 0, \tag{3.2}$$

and

$$\operatorname{Im} \left\{ \int_\Gamma \left(\left(\frac{Z}{\tau^w} \right) w \right) \overline{w} \, ds \right\} \geq 0, \tag{3.3}$$

where $\Gamma := \{r = \bar{g}\}$. The first is required to invoke Rellich's Lemma [6], while the sign on the second is necessary if the imaginary part of $\epsilon^{(w)}$ is greater than or equal to zero.

Remark 3.1. We point out that since $\tau^u \in \mathbf{R}^+$ the choice of Despres [8], $Y = -i\eta$ where $\eta \in \mathbf{R}^+$, satisfies (3.2). The situation with Z is more delicate as $\epsilon^{(w)}$ can be complex. More specifically, if $\epsilon^{(w)} = \epsilon^{(w)\prime} + i\epsilon^{(w)\prime\prime}$ and $Z = Z' + iZ''$, since

$$\operatorname{Im} \left\{ \frac{Z}{\tau^w} \right\} = \begin{cases} Z'', & \text{TE}, \\ \epsilon^{(w)\prime} Z'', & \text{dielectric in TM}, \\ \epsilon^{(w)\prime} Z'' + \epsilon^{(w)\prime\prime} Z', & \text{metal in TM}, \end{cases}$$

the choice of Despres [8], $Z = i\eta$ where $\eta \in \mathbf{R}^+$, satisfies (3.3) provided that the interior is not a metal ($\epsilon^{(w)\prime} < 0$ and $\epsilon^{(w)\prime\prime} > 0$) in TM polarization. In this case our choice of Z must be made specific to the material on the interior, e.g., $Z''/Z' > -\epsilon^{(w)\prime}/\epsilon^{(w)\prime\prime} > 0$, which, of course, can be accommodated.

Definition 3.2. *Given Y satisfying (3.2) and a sufficiently smooth and small deformation $g(\theta)$, the unique periodic solution of*

$$\Delta u + (k^u)^2 u = 0, \qquad \bar{g} + g(\theta) < r < R^{(u)}, \tag{3.4a}$$

$$-\tau^u \partial_N u + Y u = U, \qquad r = \bar{g} + g(\theta), \tag{3.4b}$$

$$\partial_r u + T^{(u)}[u] = 0, \qquad r = R^{(u)}, \tag{3.4c}$$

defines the Impedance–Impedance Operator

$$Q[U] := \tilde{U}. \tag{3.5}$$

Definition 3.3. *Given Z satisfying (3.3) and a sufficiently smooth and small deformation $g(\theta)$, the unique periodic solution of*

$$\Delta w + (k^w)^2 w = 0, \qquad R^{(w)} < r < \bar{g} + g(\theta), \tag{3.6a}$$

$$\tau^w \partial_N w - Zw = W, \qquad r = \bar{g} + g(\theta), \tag{3.6b}$$

$$\partial_r w - T^{(w)}[w] = 0, \qquad r = R^{(w)}, \tag{3.6c}$$

defines the Impedance–Impedance Operator

$$S[W] := \tilde{W}. \tag{3.7}$$

In terms of these operators the boundary conditions, (3.1), become

$$U + S[W] = \zeta, \quad Q[U] + W = \psi,$$

or

$$\begin{pmatrix} I & S \\ Q & I \end{pmatrix} \begin{pmatrix} U \\ W \end{pmatrix} = \begin{pmatrix} \zeta \\ \psi \end{pmatrix}. \tag{3.8}$$

For later use, we write this more compactly as

$$\mathbf{A}\mathbf{V} = \mathbf{F}, \tag{3.9}$$

where

$$\mathbf{A} = \begin{pmatrix} I & S \\ Q & I \end{pmatrix}, \quad \mathbf{V} = \begin{pmatrix} U \\ W \end{pmatrix}, \quad \mathbf{F} = \begin{pmatrix} \zeta \\ \psi \end{pmatrix}. \tag{3.10}$$

3.1. A High–Order Perturbation of Surfaces Method.

Our approach to simulating solutions to (3.9) is perturbative in nature and based upon the assumption that $g(\theta) = \varepsilon f(\theta)$ where ε is sufficiently small. However, this can be relaxed to include *all* $\varepsilon \in \mathbf{R}$ up to topological obstruction via the method outlined in [33]. As we shall show in Section 6, provided that f is sufficiently smooth (which we shall make more precise later), then the IIOs, Q and S, are analytic in the perturbation parameter ε so that the following expansions are strongly convergent in an appropriate Sobolev space

$$Q(\varepsilon f) = \sum_{n=0}^{\infty} Q_n(f)\varepsilon^n, \quad S(\varepsilon f) = \sum_{n=0}^{\infty} S_n(f)\varepsilon^n. \tag{3.11}$$

Clearly, if this is the case then the operator $\mathbf{A}$ will also be analytic, as will $\mathbf{F}$ so that

$$\{\mathbf{A}(\varepsilon f), \mathbf{F}(\varepsilon f)\} = \sum_{n=0}^{\infty} \{\mathbf{A}_n(f), \mathbf{F}_n(f)\}\varepsilon^n. \tag{3.12}$$

We will shortly show that, under certain circumstances, there will be a unique solution, $\mathbf{V}$, of (3.9) which is also analytic in ε

$$\mathbf{V}(\varepsilon f) = \sum_{n=0}^{\infty} \mathbf{V}_n(f)\varepsilon^n. \tag{3.13}$$

Furthermore, it is clear that the $\mathbf{V}_n$ must satisfy

$$\mathbf{V}_n = \mathbf{A}_0^{-1} \left\{ \mathbf{F}_n - \sum_{\ell=0}^{n-1} \mathbf{A}_{n-\ell} \mathbf{V}_\ell \right\}, \tag{3.14}$$

and one key in the analysis is the invertibility of the operator $\mathbf{A}_0$ which we now investigate.

3.2. The Trivial Configuration: LSPR Condition. To investigate this invertibility question we show how our formulation delivers the classical solution for plane wave scattering by a cylindrical obstacle. For this we consider (3.8) in the case $g \equiv 0$,

$$\begin{pmatrix} I & S_0 \\ Q_0 & I \end{pmatrix} \begin{pmatrix} U \\ W \end{pmatrix} = \begin{pmatrix} \zeta_0 \\ \psi_0 \end{pmatrix}. \tag{3.15}$$

As we shall presently see, the operators Q_0 and S_0 are (order–one) Fourier multipliers. Recall that a Fourier multiplier $m(D)$ is defined by

$$m(D)[\xi(x)] := \sum_{p=-\infty}^{\infty} m(p) \hat{\xi}_p e^{ip\theta},$$

so that, e.g., $\partial_x = iD$. In this trivial configuration, the solutions to (3.4) and (3.6) are, (c.f. (2.2)),

$$u(r,\theta) = \sum_{p=-\infty}^{\infty} \frac{\hat{U}_p}{-\tau^u (k^u \bar{g}) H_p'(k^u \bar{g}) + \hat{Y}_p H_p(k^u \bar{g})} H_p(k^u r) e^{ip\theta},$$

$$w(r,\theta) = \sum_{p=-\infty}^{\infty} \frac{\hat{W}_p}{\tau^w (k^w \bar{g}) J_p'(k^u \bar{g}) - \hat{Z}_p J_p(k^w \bar{g})} J_p(k^w r) e^{ip\theta},$$

respectively. From these we find for (3.5)

$$\begin{aligned} Q_0[U] &= \sum_{p=-\infty}^{\infty} \widehat{(Q_0)}_p \hat{U}_p e^{ip\theta} = \sum_{p=-\infty}^{\infty} \left(\frac{-\tau^u (k^u \bar{g}) H_p'(k^u \bar{g}) + \hat{Z}_p H_p(k^u \bar{g})}{-\tau^u (k^u \bar{g}) H_p'(k^u \bar{g}) + \hat{Y}_p H_p(k^u \bar{g})} \right) \hat{U}_p e^{ip\theta} \\ &=: \left(\frac{-\tau^u (k^u \bar{g}) H_D'(k^u \bar{g}) + Z H_D(k^u \bar{g})}{-\tau^u (k^u \bar{g}) H_D'(k^u \bar{g}) + Y H_D(k^u \bar{g})} \right) U, \end{aligned}$$

and for (3.7)

$$\begin{aligned} S_0[W] &= \sum_{p=-\infty}^{\infty} \widehat{(S_0)}_p \hat{W}_p e^{ip\theta} = \sum_{p=-\infty}^{\infty} \left(\frac{\tau^w (k^w \bar{g}) J_p'(k^w \bar{g}) - \hat{Y}_p J_p(k^w \bar{g})}{\tau^w (k^w \bar{g}) J_p'(k^w \bar{g}) - \hat{Z}_p J_p(k^w \bar{g})} \right) \hat{W}_p e^{ip\theta} \\ &=: \left(\frac{\tau^w (k^w \bar{g}) J_D'(k^w \bar{g}) - Y J_D(k^w \bar{g})}{\tau^w (k^w \bar{g}) J_D'(k^w \bar{g}) - Z J_D(k^w \bar{g})} \right) W, \end{aligned}$$

which define the order–one Fourier multipliers

$$Q_0 = \left(\frac{-\tau^u (k^u \bar{g}) H_D'(k^u \bar{g}) + Z H_D(k^u \bar{g})}{-\tau^u (k^u \bar{g}) H_D'(k^u \bar{g}) + Y H_D(k^u \bar{g})} \right), \tag{3.16a}$$

$$S_0 = \left(\frac{\tau^w (k^w \bar{g}) J_D'(k^w \bar{g}) - Y J_D(k^w \bar{g})}{\tau^w (k^w \bar{g}) J_D'(k^w \bar{g}) - Z J_D(k^w \bar{g})} \right), \tag{3.16b}$$

respectively.

Returning to (3.15) we find the solution at each wavenumber is given by

$$\begin{pmatrix} \hat{U}_p \\ \hat{W}_p \end{pmatrix} = \frac{1}{1 - \widehat{(S_0)}_p \widehat{(Q_0)}_p} \begin{pmatrix} 1 & -\widehat{(S_0)}_p \\ -\widehat{(Q_0)}_p & 1 \end{pmatrix} \begin{pmatrix} \widehat{(\zeta_0)}_p \\ \widehat{(\psi_0)}_p \end{pmatrix}, \tag{3.17}$$

and it is clear that unique solvability of this system hinges on the determinant function

$$\Delta_p := 1 - \widehat{(S_0)}_p \widehat{(Q_0)}_p. \tag{3.18}$$

With the notation

$$\mathbf{J} = J_p(k^w \bar{g}), \quad \mathbf{J}' = \tau^w(k^w \bar{g}) J_p'(k^w \bar{g}), \quad \mathbf{H} = H_p(k^u \bar{g}), \quad \mathbf{H}' = -\tau^u(k^u \bar{g}) H_p'(k^u \bar{g}),$$

we find

$$\Delta_p = \frac{(Y - Z)(\mathbf{J}'\mathbf{H} - \mathbf{J}\mathbf{H}')}{(\mathbf{H}' + Y\mathbf{H})(\mathbf{J}' - Z\mathbf{J})}.$$

The zeros of this function are the same as those we found in [37], and thus deliver the same result in the "small radius" (quasi–static) limit [23], $k^u \bar{g} \ll 1$ and $k^w \bar{g} \ll 1$,

$$\epsilon^{(u)} = -\mathrm{Re}\left\{ \epsilon^{(w)} \right\} - i\mathrm{Im}\left\{ \epsilon^{(w)} \right\}.$$

If the Fröhlich condition, c.f. (1.1), $\epsilon^{(u)} = -\mathrm{Re}\left\{ \epsilon^{(w)} \right\}$, is verified then it can "almost" be true. Again, this is *different* from the three dimensional Fröhlich condition for nanoparticles [23], $\epsilon^{(u)} = -2\mathrm{Re}\left\{ \epsilon^{(w)} \right\}$.

Remark 3.4. At this point we might worry that the function Δ_p could be zero. However, a good deal is known about the unique solvability of the scattering problem in this trivial configuration, (3.15). Moiola and Spence [24] provide an excellent summary of the state–of–the–art and a discussion of known results. Rather than reproduce their extensive exposition, we simply restrict ourselves to a configuration

$$(k^u, k^w, \bar{g}, Y, Z) \text{ such that (3.15) admits a unique solution.} \tag{3.19}$$

4. Interfacial Function Spaces.

We begin with a careful mathematical analysis of (3.9) which will help justify the computational results we present in Section 7. Before describing these rigorous results we specify the interfacial function spaces we require. For any real $s \geq 0$ we recall the classical, periodic, L^2–based Sobolev norm [19]

$$\|U\|_{H^s}^2 := \sum_{p=-\infty}^{\infty} \langle p \rangle^{2s} \left| \hat{U}_p \right|^2, \quad \langle p \rangle^2 := 1 + |p|^2, \quad \hat{U}_p := \frac{1}{2\pi} \int_0^{2\pi} U(\theta) e^{ipx} \, d\theta, \tag{4.1}$$

which gives rise to the periodic Sobolev space [19]

$$H^s([0, 2\pi]) := \left\{ U(x) \in L^2([0, 2\pi]) \mid \|U\|_{H^s} < \infty \right\}.$$

We also require the dual space of $H^s([0, 2\pi])$ which is characterized by Theorem 8.10 of [19] and is typically denoted $H^{-s}([0, 2\pi])$.

With this definition it is a simple matter to prove the following Lemma.

LEMMA 4.1. *For any $s \in \mathbf{R}$ there exist constants $C_Q, C_S > 0$ such that*

$$\|Q_0 U\|_{H^s} \leq C_Q \|U\|_{H^s}, \quad \|S_0 W\|_{H^s} \leq C_S \|W\|_{H^s},$$

for any $U, W \in H^s$.

We also recall, for any integer $s \geq 0$, the space of s–times continuously differentiable functions with the Hölder norm $|f|_{C^s} = \max_{0 \leq \ell \leq s} \left|\partial_x^\ell f\right|_{L^\infty}$. For later reference we recall the following classical result.

LEMMA 4.2. *For any integer $s \geq 0$, any $\beta > 0$, and any set $U \subset \mathbf{R}^m$, if $f, u, g, \mu : U \to \mathbf{C}$, $f \in C^s(U)$, $u \in H^s(U)$, $g \in C^{s+1/2+\beta}(U)$, $\mu \in H^{s+1/2}(U)$, then*

$$\|fu\|_{H^s} \leq \tilde{M}(m, s, U) |f|_{C^s} \|u\|_{H^s}, \quad \|g\mu\|_{H^{s+1/2}} \leq \tilde{M}(m, s, U) |g|_{C^{s+1/2+\beta}} \|\mu\|_{H^{s+1/2}},$$

for some constant $\tilde{M}$.

In addition, we require the analogous result valid for *any* real value of s [12, 30].

LEMMA 4.3. *For any $s \in \mathbf{R}$ and any set $U \subset \mathbf{R}^m$, if $\varphi, \psi : U \to \mathbf{C}$, $\varphi \in H^{|s|+m+2}(U)$ and $\psi \in H^s(U)$, then*

$$\|\varphi\psi\|_{H^s} \leq M(m, s, U) \|\varphi\|_{H^{|s|+m+2}} \|\psi\|_{H^s},$$

for some constant M.

Remark 4.4. Presently we will be required to estimate terms of the form

$$\|(\partial_\theta f)u\|_{L^2(\Omega)} = \|(\partial_\theta f)u\|_{H^0(\Omega)}, \quad \|(\partial_\theta f)\mu\|_{H^{-1/2}([0,2\pi])},$$

where $\Omega \subset \mathbf{R}^2$, which feature Sobolev norms too weak for the standard algebra estimate, Lemma 4.2. For this reason we have introduced Lemma 4.3 which allows us to compute, for $m = 2$,

$$\begin{aligned}
\|(\partial_\theta f)u\|_{L^2(\Omega)} = \|(\partial_\theta f)u\|_{H^0(\Omega)} &\leq M \|\partial_\theta f\|_{H^{|0|+2+2}([0,2\pi])} \|u\|_{H^0(\Omega)} \\
&\leq M \|f\|_{H^5([0,2\pi])} \|u\|_{H^0(\Omega)},
\end{aligned}$$

while, for $m = 1$,

$$\begin{aligned}
\|(\partial_\theta f)\mu\|_{H^{-1/2}([0,2\pi])} &\leq M \|\partial_\theta f\|_{H^{|-1/2|+1+2}([0,2\pi])} \|\mu\|_{H^{-1/2}([0,2\pi])} \\
&\leq M \|f\|_{H^{4+1/2}([0,2\pi])} \|\mu\|_{H^{-1/2}([0,2\pi])}.
\end{aligned}$$

In this way, if we require $f \in H^5([0, 2\pi])$ then we can use the algebra property of Lemma 4.3 throughout our developments. We note that, by Sobolev embedding, if $f \in H^5([0, 2\pi])$ then $f \in C^4([0, 2\pi])$, and if $f \in C^5([0, 2\pi])$ then $f \in H^5([0, 2\pi])$.

5. Analyticity of Solutions. We can now take up the rigorous analysis of (3.13) for which we utilize the general theory of analyticity of solutions of linear systems of equations. To be more specific, we follow the developments found in [28] for the solution of (3.9). Given the expansions (3.12) we seek the solution of the form (3.13) which satisfy (3.14). We restate the main result here for completeness.

THEOREM 5.1 (Nicholls [28]). *Given two Banach spaces $\mathcal{X}$ and $\mathcal{Y}$, suppose that:*

(H1) $\mathbf{F}_n \in \mathcal{Y}$ for all $n \geq 0$, and there exist constants $C_F > 0$, $B_F > 0$ such that

$$\|\mathbf{F}_n\|_{\mathcal{Y}} \leq C_F B_F^{\ n}, \quad n \geq 0.$$

(H2) $\mathbf{A}_n : \mathcal{X} \to \mathcal{Y}$ *for all* $n \geq 0$, *and there exists constants* $C_A > 0$, $B_A > 0$ *such that*

$$\|\mathbf{A}_n\|_{\mathcal{X}\to\mathcal{Y}} \leq C_A B_A^n, \quad n \geq 0.$$

(H3) $\mathbf{A}_0^{-1} : \mathcal{Y} \to \mathcal{X}$, *and there exists a constant* $C_e > 0$ *such that*

$$\left\|\mathbf{A}_0^{-1}\right\|_{\mathcal{Y}\to\mathcal{X}} \leq C_e.$$

Then the equation (3.9) *has a unique solution* (3.13), *and there exist constants* $C_V > 0$ *and* $B_V > 0$ *such that*

$$\|\mathbf{V}_n\|_{\mathcal{X}} \leq C_V B_V^n, \quad n \geq 0,$$

for any $C_V \geq 2C_eC_R$, $B_V \geq \max\{B_F, 2B_A, 4C_eC_AB_A\}$, *which implies that, for any* $0 \leq \rho < 1$, (3.13) *converges for all* ε *such that* $B_V\varepsilon < \rho$, *i.e.,* $\varepsilon < \rho/B_V$.

All that remains is to find the forms (3.12), and establish Hypotheses (H1), (H2), and (H3). For the former it is quite clear from (3.9) that

$$\mathbf{A}_0 = \begin{pmatrix} I & S_0 \\ Q_0 & I \end{pmatrix}, \quad \mathbf{A}_n = \begin{pmatrix} 0 & S_n \\ Q_n & 0 \end{pmatrix}, \quad n \geq 1,$$
$$\mathbf{V}_n = \begin{pmatrix} U_n \\ W_n \end{pmatrix}, \quad \mathbf{F}_n = \begin{pmatrix} \zeta_n \\ \psi_n \end{pmatrix}.$$

For the spaces $\mathcal{X}$ and $\mathcal{Y}$, the natural choices for the weak formulation we pursue here are $\mathcal{X} = \mathcal{Y} = H^{-1/2}([0,2\pi]) \times H^{-1/2}([0,2\pi])$, so that

$$\left\|\begin{pmatrix} U \\ W \end{pmatrix}\right\|_{\mathcal{X}}^2 = \|U\|_{H^{-1/2}}^2 + \|W\|_{H^{-1/2}}^2.$$

Hypothesis (H1): We begin by noting that

$$\zeta_n = \tau^u \nu_n + Y\xi_n, \quad \psi_n = -\tau^u \nu_n + Z\xi_n,$$

where

$$\xi_n = -e^{ik^u \bar{g}\sin(\phi-\theta)} \left[(ik^u)\sin(\phi-\theta)\right]^n F_n, \quad F_n := \frac{f^n}{n!},$$
$$\nu_n = \bar{g}\left[(ik^u)\sin(\phi-\theta)\right]\xi_n + (ik^u)\left[f\sin(\phi-\theta) + (\partial_\theta f)\cos(\phi-\theta)\right]\xi_{n-1}.$$

Now, if $Y : H^{1/2} \to H^{-1/2}$ and $Z : H^{1/2} \to H^{-1/2}$, then

$$\|R_n\|_{\mathcal{Y}}^2 = \|\zeta_n\|_{H^{-1/2}}^2 + \|\psi_n\|_{H^{-1/2}}^2 \leq 2\left|\tau^u\right|^2 \|\nu_n\|_{H^{-1/2}}^2 + (C_Y + C_Z)\|\xi_n\|_{H^{1/2}}^2,$$

and, from the explanation given in Remark 4.4, this will be bounded provided that $f \in H^5([0,2\pi])$.

Hypothesis (H2): The analyticity estimates for the IIOs Q, Theorem 6.4, and S, Theorem 6.1, show rather directly that Hypothesis (H2) is verified provided that Y and Z satisfy (3.2) and (3.3), respectively. Indeed, as we have

$$\|Q_n[U]\|_{H^{-1/2}} \leq C_Q B_Q^n, \quad \|S_n[W]\|_{H^{-1/2}} \leq C_S B_S^n,$$

it is a straightforward matter to show that $\|\mathbf{A}_n\|_{\mathcal{X}\to\mathcal{Y}} \le C_A B_A^n$, for $C_A = \max\{C_Q, C_S\}$ and $B_A = \max\{B_Q, B_S\}$.

Hypothesis (H3): We now address the existence and invertibility properties of the linearized operator $\mathbf{A}_0$ in the following Lemma.

Lemma 5.2. *If $\zeta, \psi \in H^{-1/2}([0, 2\pi])$, Y satsisfies (3.2), and Z satisfies (3.3), then there exists a unique solution of*

$$\begin{pmatrix} I & S_0 \\ Q_0 & I \end{pmatrix} \begin{pmatrix} U \\ W \end{pmatrix} = \begin{pmatrix} \zeta \\ \psi \end{pmatrix},$$

c.f. (3.15), satisfying

$$\|U\|_{H^{-1/2}} \le \tilde{C}_e \left\{ \|\zeta\|_{H^{-1/2}} + \|\psi\|_{H^{-1/2}} \right\},$$
$$\|W\|_{H^{-1/2}} \le \tilde{C}_e \left\{ \|\zeta\|_{H^{-1/2}} + \|\psi\|_{H^{-1/2}} \right\},$$

for some universal constant $\tilde{C}_e > 0$.

Proof. The bulk of the proof has already been worked out in Section 3.2. If we expand

$$\zeta(\theta) = \sum_{p=-\infty}^{\infty} \hat{\zeta}_p e^{ip\theta}, \quad \psi(\theta) = \sum_{p=-\infty}^{\infty} \hat{\psi}_p e^{ip\theta},$$

then we can find solutions of (3.15)

$$U(\theta) = \sum_{p=-\infty}^{\infty} \hat{U}_p e^{ip\theta}, \quad W(\theta) = \sum_{p=-\infty}^{\infty} \hat{W}_p e^{ip\theta},$$

where

$$\begin{pmatrix} \hat{U}_p \\ \hat{W}_p \end{pmatrix} = \frac{1}{1 - \widehat{(S_0)}_p \widehat{(Q_0)}_p} \begin{pmatrix} 1 & -\widehat{(S_0)}_p \\ -\widehat{(Q_0)}_p & 1 \end{pmatrix} \begin{pmatrix} \widehat{(\zeta_0)}_p \\ \widehat{(\psi_0)}_p \end{pmatrix},$$

c.f. (3.17). The key is the analysis of the operators $\widehat{(S_0)}_p$, $\widehat{(Q_0)}_p$, and the determinant function $\Delta_p = 1 - \widehat{(S_0)}_p \widehat{(Q_0)}_p$, c.f. (3.18). For these, given our hypothesis (3.19) and their asymptotic properties, it is not difficult to show that there exist constants $\tilde{K}_Q, \tilde{K}_S, \tilde{K}_\Delta > 0$ such that

$$\left| \widehat{(Q_0)}_p \right| < \tilde{K}_Q, \quad \left| \widehat{(S_0)}_p \right| < \tilde{K}_S, \quad \frac{1}{|\Delta_p|} < \tilde{K}_\Delta.$$

With these we can estimate

$$\|U\|_{H^{-1/2}}^2 = \sum_{p=-\infty}^{\infty} \langle p \rangle^{-1} \left| \hat{U}_p \right|^2 < \sum_{p=-\infty}^{\infty} \langle p \rangle^{-1} \tilde{K}_\Delta^2 \left(\left| \hat{\zeta}_p \right|^2 + \tilde{K}_S^2 \left| \hat{\psi}_p \right|^2 \right)$$
$$= \tilde{K} \left(\|\zeta\|_{H^{-1/2}}^2 + \|\psi\|_{H^{-1/2}}^2 \right),$$

for some $\tilde{K} > 0$. Proceeding similarly for W we complete the proof. ∎

Having established Hypotheses (H1), (H2), and (H3) we can invoke Theorem 5.1 to discover our final result.

Theorem 5.3. *If $f \in H^5([0,2\pi])$, Y satisfies (3.2), and Z satisfies (3.3), then there exists a unique solution pair, (3.13), of the problem, (3.9), satisfying*

$$\|U_n\|_{H^{-1/2}} \leq C_U D^n, \quad \|W_n\|_{H^{-1/2}} \leq C_W D^n, \quad n \geq 0,$$

for any $D > \|f\|_{H^5}$, where C_U and C_W are universal constants.

6. Analyticity of the Impedance–Impedance Operators. At this point the only remaining task is to establish the analyticity of the IIOs, Q and S. In the exterior this has been accomplished for the DNO in [30] and the results are quite similar. However, the theory for the interior domain is quite different due to the Dirichlet eigenvalues on $\{r \leq \bar{g}\}$ which can render their DNOs non–existent. For this reason we focus on the interior domain.

Theorem 6.1. *If $f \in H^5([0,2\pi])$, Z satisfies (3.3), and $W \in H^{-1/2}([0,2\pi])$, then the series (3.11) converges strongly as an operator from $H^{-1/2}([0,2\pi])$ to $H^{-1/2}([0,2\pi])$. In other words there exist constants $K_S > 0$ and $B_S > 0$ such that*

$$\|S_n(f)[W]\|_{H^{-1/2}} \leq K_S B_S^n. \tag{6.1}$$

We establish this result with the method of Transformed Field Expansions (TFE) [31, 32, 33] which has proven quite successful in establishing analyticity of DNOs in similar settings [29, 30, 36]. The TFE method proceeds by effecting a domain–flattening change of variables prior to perturbation expansion. On the interior domain the relevant change of variables is

$$r' = \left\{ (\bar{g} - R^{(w)})r + R^{(w)} g(\theta) \right\} / \left\{ \bar{g} + g(\theta) - R^{(w)} \right\}, \quad \theta' = \theta,$$

which maps the perturbed domain $\{R^{(w)} < r < \bar{g} + g(\theta)\}$ to the separable one $\Omega_{R^{(w)},\bar{g}} = \{R^{(w)} < r' < \bar{g}\}$. This transformation changes the field w to

$$v(r',\theta') := w(\{(\bar{g} + g(\theta') - R^{(w)})r' - R^{(w)} g(\theta')\}/\{\bar{g} - R^{(w)}\}, \theta'),$$

and modifies (A.4) to

$$\Delta v + (k^w)^2 v = F(r,\theta;g), \qquad R^{(w)} < r < \bar{g}, \tag{6.2a}$$

$$\tau^w \partial_N v - Z v = W(\theta) + l(\theta;g), \qquad r = \bar{g}, \tag{6.2b}$$

$$\partial_r v - T^{(w)}[v] = h(\theta;g), \qquad r = R^{(w)}, \tag{6.2c}$$

where we have dropped the primed notation for clarity. The forms for F, l, and h are not difficult to derive, and they can be deduced from their expansions which we present in (6.5).

Upon setting $g = \varepsilon f$ and expanding

$$v(r,\theta,\varepsilon) = \sum_{n=0}^{\infty} v_n(r,\theta)\varepsilon^n, \tag{6.3}$$

we can show that

$$\Delta v_n + (k^w)^2 v_n = F_n, \qquad R^{(w)} < r < \bar{g}, \tag{6.4a}$$

$$\partial_r v_n - \frac{Z}{\tau^w \bar{g}} v_n = \delta_{n,0} \frac{W}{\tau^w \bar{g}} + l_n, \qquad r = \bar{g}, \tag{6.4b}$$

$$\partial_r v_n - T^{(w)}[v_n] = h_n, \qquad r = R^{(w)}, \tag{6.4c}$$

where, $\delta_{n,m}$ is the Kronecker delta, and

$$F_n = -\frac{1}{(\bar{g} - R^{(w)})^2} \left[F_n^{(0)} + \partial_r F_n^{(r)} + \partial_\theta F_n^{(\theta)} \right], \tag{6.5a}$$

$$F_n^{(0)} = -(\bar{g} - R^{(w)}) f (r - R^{(w)}) \partial_r v_{n-1} + \dots, \tag{6.5b}$$

$$F_n^{(r)} = 2(\bar{g} - R^{(w)}) f r (r - R^{(w)}) \partial_r v_{n-1} + \dots, \tag{6.5c}$$

$$F_n^{(\theta)} = -f f' (r - R^{(w)}) \partial_r v_{n-2} + \dots, \tag{6.5d}$$

$$l_n = -(1/\bar{g}^2)(f')^2 \partial_r v_{n-2} + \dots, \tag{6.5e}$$

$$h_n = \frac{f}{\bar{g} - R^{(w)}} T^{(w)} [v_{n-1}], \tag{6.5f}$$

are the n–th order terms in the Taylor series expansions of F, l, and h, respectively. Furthermore, $F_n^{(0)}$, $F_n^{(r)}$, and $F_n^{(\theta)}$ are, in order, the undifferentiated, radial derivative, and angular derivative portions of F_n.

In addition, the IIO S, (3.7), can be stated in transformed coordinates. If we then expand S in ε, (3.11), the n–th term in the expansion can be expressed as

$$S_n[W] = \tau^w \left\{ -\frac{f(f')}{\bar{g}(\bar{g} - R^{(w)})} \partial_\theta v_{n-2} \right\} + \dots, \tag{6.6}$$

so that, provided with estimates on the $\{v_n\}$, we can control the terms, $\{S_n\}$.

Our main result is the following analyticity theorem.

THEOREM 6.2. *If $f \in H^5([0, 2\pi])$, Z satisfies (3.3), and $W \in H^{-1/2}([0, 2\pi])$, then the series (6.3) converges strongly. In other words there exist constants $K_v > 0$ and $B_S > 0$ such that*

$$\|v_n\|_{H^1} \leq K_v B_S^n. \tag{6.7}$$

The proof of Theorem 6.2 proceeds by applying an elliptic estimate, Theorem A.1, to (6.4) followed by a recursive result, Lemma 6.3. To control the right hand side of (6.4) we prove the following.

LEMMA 6.3. *Suppose that $f \in H^5([0, 2\pi])$ and Z satisfies (3.3). Assume that*

$$\|v_n\|_{H^1(\Omega_{R^{(w)},\bar{g}})} \leq K_v B_S^n, \quad \forall n < N,$$

for constants $K_v > 0$ and $B_S > 0$, then there exists a constant $C_v > 0$ such that

$$\max \left\{ \|F_N\|_{(H^1(\Omega_{R^{(w)},\bar{g}}))'}, \|h_N\|_{H^{-1/2}([0,2\pi])}, \|l_N\|_{H^{-1/2}([0,2\pi])} \right\} \\ \leq C_v K_v \left(\|f\|_{H^5} B_S^{N-1} + \|f\|_{H^5}^2 B_S^{N-2} \right).$$

Proof. Note that from (6.5) and the definition of $(H^1)'$ [11]

$$\|F_N\|_{(H^1)'} \leq \left\| F_N^{(0)} \right\|_{L^2} + \left\| F_N^{(r)} \right\|_{L^2} + \left\| F_N^{(\theta)} \right\|_{L^2},$$

and, for conciseness, we consider only one term from $F_N^{(\theta)}$,

$$\mathcal{F}_N^{(\theta)} := -f f' (r - R^{(w)}) \partial_r v_{N-2};$$

the rest can be treated in a similar fashion. For this we estimate, using Lemma 4.3,

$$\begin{aligned}\left\|\mathcal{F}_N^{(\theta)}\right\|_{L^2} &\leq \left\|-ff'(r-R^{(w)})\partial_r v_{N-2}\right\|_{L^2} \leq M\|f\|_{H^4} M\|f\|_{H^5}\mathcal{R}\|v_{N-2}\|_{H^1} \\ &\leq M^2\|f\|_{H^5}^2 \mathcal{R}K_v B_S^{N-2},\end{aligned}$$

where $\mathcal{R}$ is defined by $\left\|(r-R^{(w)})v\right\|_{L^2} \leq \mathcal{R}\|v\|_{L^2}$, and we are done if C_v is chosen appropriately.

For h_N we conduct the following sequence of steps

$$\begin{aligned}\|h_N\|_{H^{-1/2}} &\leq \left\|\frac{f}{\bar{g}-R^{(w)}}T^{(w)}\left[v_{N-1}\right]\right\|_{H^{-1/2}} \leq \frac{M}{\bar{g}-R^{(w)}}\|f\|_{H^{3+1/2}}\left\|T^{(w)}\left[v_{N-1}\right]\right\|_{H^{-1/2}} \\ &\leq \frac{M}{\bar{g}-R^{(w)}}\|f\|_{H^5} C_{T^{(w)}}\|v_{N-1}\|_{H^{1/2}} \leq \frac{MC_{T^{(w)}}}{\bar{g}-R^{(w)}}\|f\|_{H^5} C_t\|v_{N-1}\|_{H^1} \\ &\leq \frac{MC_{T^{(w)}}}{\bar{g}-R^{(w)}}\|f\|_{H^5} C_t K_v B_S^{N-1},\end{aligned}$$

where $C_{T^{(w)}}$ is the bounding constant for the operator $T^{(w)}$, and C_t is the bounding constant for the trace operator $\|v\|_{H^{1/2}([0,2\pi])} \leq C_t\|v\|_{H^1(\Omega_{R^{(w)},\bar{g}})}$. We are done if we select C_v large enough.

Regarding the terms l_N, we once again focus on a single term

$$\mathcal{L}_N := -(1/\bar{g}^2)(f')^2\partial_r v_{N-2},$$

and make the estimates

$$\begin{aligned}\|\mathcal{L}_N\|_{H^{-1/2}} &= \left\|-\frac{1}{\bar{g}^2}(f')^2\partial_r v_{N-2}\right\|_{H^{-1/2}} \leq \frac{M^2}{\bar{g}^2}\|f\|_{H^{4+1/2}}^2\|\partial_r v_{N-2}\|_{H^{-1/2}} \\ &\leq \frac{M^2}{\bar{g}^2}\|f\|_{H^{4+1/2}}^2 C_t\|v_{N-2}\|_{H^1} \leq \frac{M^2C_t}{\bar{g}^2}\|f\|_{H^5}^2 K_v B_S^{N-2},\end{aligned}$$

and we are done if C_v is chosen well. ∎

We can now present the proof of Theorem 6.2.

Proof. (Theorem 6.2). We work by induction and begin with $n=0$. The estimate on v_0 follows directly from Theorem A.2 with F and L identically zero. We now assume that (6.7) holds for all $n<N$ and apply Theorem A.2 which implies that

$$\|v_N\|_{H^1} \leq C_e\left\{\|F_N\|_{(H^1)'} + \|l_N\|_{H^{-1/2}} + \|h_N\|_{H^{-1/2}}\right\}.$$

Using Lemma 6.3 we have

$$\|v_N\|_{H^1} \leq C_e 3C_v K_v\left\{\|f\|_{H^5} B_S^{N-1} + \|f\|_{H^5}^2 B_S^{N-2}\right\} \leq K_v B_S^N,$$

provided that we choose $3C_eC_v\|f\|_{H^5} < B_S/2$, $3C_eC_v\|f\|_{H^5}^2 < B_S^2/2$, which can be ensured by demanding $B_S > \max\left\{6C_eC_v, \sqrt{6C_eC_v}\right\}\|f\|_{H^5}$. ∎

Finally, we are in a position to establish Theorem 6.1.

Proof. (Theorem 6.1). From (6.6) and applying Theorem 6.2, it is straightforward to see that

$$\begin{aligned}\|S_0(f)[W]\|_{H^{-1/2}} &\leq \|\tau^w\bar{g}\partial_r v_0 - Yv_0\|_{H^{-1/2}} \leq \|\tau^w\bar{g}\partial_r v_0\|_{H^{-1/2}} + \|Yv_0\|_{H^{-1/2}} \\ &\leq |\tau^w|\,\bar{g}\,\|v_0\|_{H^{1/2}} + C_Y\|v_0\|_{H^{1/2}} \leq (|\tau^w|\,\bar{g}+C_Y)\,C_t\|v_0\|_{H^1} \\ &\leq (|\tau^w|\,\bar{g}+C_Y)\,C_tK_v \leq K_S,\end{aligned}$$

if $K_S > 0$ is chosen appropriately.

Assuming that (6.1) holds for all $n < N$ we now investigate an estimate of S_N. For simplicity we consider the single term

$$\mathcal{S}_N := \tau^w \left(\frac{-ff'}{\bar{g}(\bar{g} - R^{(w)})} \right) \partial_\theta v_{N-2}$$

and we measure

$$\begin{aligned}
\|\mathcal{S}_N\|_{H^{-1/2}} &\leq \left\| \tau^w \left(\frac{-ff'}{\bar{g}(\bar{g} - R^{(w)})} \right) \partial_\theta v_{N-2} \right\|_{H^{-1/2}} \\
&\leq |\tau^w| \frac{M^2}{\bar{g}(\bar{g} - R^{(w)})} \|f\|^2_{H^{4+1/2}} \|\partial_\theta v_{N-2}\|_{H^{-1/2}} \\
&\leq |\tau^w| \frac{M^2}{\bar{g}(\bar{g} - R^{(w)})} \|f\|^2_{H^5} C_t \|v_{N-2}\|_{H^1} \\
&\leq |\tau^w| \frac{M^2}{\bar{g}(\bar{g} - R^{(w)})} \|f\|^2_{H^5} C_t K_v B_S^{N-2}.
\end{aligned}$$

We are done provided that we choose $K_S > |\tau^w| M^2/(\bar{g}(\bar{g} - R^{(w)}))C_t K_v$, and $B_S > \|f\|_{H^5}$. ∎

In an analgous manner, the analyticity of Q can be established. The only significant change is the requirement that Theorem A.1 is required rather than Theorem A.2.

THEOREM 6.4. *If $f \in H^5([0, 2\pi])$, Y satisfies (3.2), and $U \in H^{-1/2}([0, 2\pi])$ then the series (3.11) converges strongly as an operator from $H^{-1/2}([0, 2\pi])$ to $H^{-1/2}([0, 2\pi])$. In other words there exist constants $K_Q > 0$ and $B_Q > 0$ such that*

$$\|Q_n(f)[U]\|_{H^{-1/2}} \leq K_Q B_Q^n.$$

7. Numerical Results.

We now present results of simulations of our implementations of the algorithms outlined above. The schemes are essentially High–Order Spectral (HOS) [13, 9] with nonlinearities approximated by convolutions implemented with the Fast Fourier Transform algorithm.

7.1. Implementation Details.

The numerical approaches we describe in this section utilize either the Dirichlet–Neumann operator (DNO) formulation of the problem [37] or its IIO alternative specified in (3.8). The relevant operators (DNO and IIO, respectively) are simulated using the TFE methodology [31, 33, 34]. The TFE method is a Fourier collocation/Taylor method [32, 34] enhanced by Padé summation [2]. In more detail, for the IIO S we approximate W by

$$W^{N_\theta,N}(\theta) := \sum_{n=0}^{N} \sum_{p=-N_\theta/2}^{N_\theta/2-1} \hat{W}_{n,p} e^{ip\theta} \varepsilon^n,$$

and insert this into (3.14) for $0 \leq n \leq N$ to determine approximation $v_n^{N_\theta,N_r,N}(r, \theta)$ which are used in (6.6) to simulate the IIO. As has been pointed out in [32, 29, 37], the TFE approach requires an additional discretization in the radial direction which we achieve by a Chebyshev collocation approach. We recall that the cost of this approach will be $\mathcal{O}(N_\theta \log(N_\theta) N_r \log(N_r) N^2)$ where the final factor is due to the cost of the *formation* of the right–hand–sides, e.g. F_n, which is $\mathcal{O}(N^2)$ at order $n = N$. An important consideration is how the Taylor series in ε are summed. The classical numerical analytic continuation technique of Padé approximation [2] has been used very successsfully for HOPS methods (see, e.g., [4, 33]), and we will use it here.

7.2. The Method of Manufactured Solutions. Before proceeding to our simulation of LSPRs, we begin by demonstrating the validity of our algorithm by conducting experiments using the Method of Manufactured Solutions (MMS) [5] To be more specific we consider the 2π–periodic, outgoing solutions of the Helmholtz equation, (2.1a),

$$u^q(r,\theta) = A_u^q H_q(k^u r) e^{iq\theta}, \quad q \in \mathbf{Z}, \quad A_u^q \in \mathbf{C},$$

and their bounded counterparts for (2.1b)

$$w^q(r,\theta) = A_w^q J_q(k^w r) e^{iq\theta}, \quad q \in \mathbf{Z}, \quad A_w^q \in \mathbf{C}.$$

We select an analytic profile

$$g(\theta) = \varepsilon f(\theta) = \varepsilon e^{\cos(\theta)}, \tag{7.1}$$

and define, for any choice of the radius of the interface $\bar{g}$, the Dirichlet and Neumann traces

$$u^{\mathrm{ex}}(\theta) := u(\bar{g} + g(\theta), \theta), \quad \tilde{u}^{\mathrm{ex}}(\theta) := (-\partial_N u^{\mathrm{ex}})(\bar{g} + g(\theta), \theta),$$

and

$$w^{\mathrm{ex}}(\theta) := w(\bar{g} + g(\theta), \theta), \quad \tilde{w}^{\mathrm{ex}}(\theta) := (\partial_N w^{\mathrm{ex}})(\bar{g} + g(\theta), \theta).$$

From these we define, for any real $\eta > 0$, the impedances

$$U^{\mathrm{ex}}(\theta) := \tau^u \tilde{u}^{\mathrm{ex}} + i\eta u^{\mathrm{ex}}, \quad \tilde{U}^{\mathrm{ex}}(\theta) := \tau^u \tilde{u}^{\mathrm{ex}} - i\eta u^{\mathrm{ex}},$$

and

$$W^{\mathrm{ex}}(\theta) := \tau^w \tilde{w}^{\mathrm{ex}} + i\eta w^{\mathrm{ex}}, \quad \tilde{W}^{\mathrm{ex}}(\theta) := \tau^w \tilde{w}^{\mathrm{ex}} - i\eta w^{\mathrm{ex}}.$$

In this case $Y = i\eta$ and $Z = -i\eta$. We point out that a rather unscientific sampling of various choices for Y and Z did not yield a clearly superior result. We were somewhat surprised by this and will investigate further in future work. Consequently we left Y and Z as these Despres values for all subsequent computations. We select the following physical parameters

$$q = 2, \quad A_u^q = 2, \quad A_w^q = 1, \quad \eta = 3.4, \quad \lambda = 0.45, \quad k^u = 13.96, \quad k^w = 5.136, \tag{7.2}$$

and numerical parameters

$$N_\theta = 64, \quad N = 16, \quad N_r = 32. \tag{7.3}$$

To demonstrate the behavior of our scheme we studied four choices of $\varepsilon = 0.005, 0.01, 0.05, 0.1$. For this we supplied $\{u^{\mathrm{ex}}, w^{\mathrm{ex}}\}$ to our HOPS algorithm to simulate DNOs producing, $\{\tilde{u}^{\mathrm{approx}}, \tilde{w}^{\mathrm{approx}}\}$, and computed the relative error

$$\mathrm{Error}_{\mathrm{rel}}^{\mathrm{DNO}} = \left\{ \left| \tilde{w}^{\mathrm{ex}} - \tilde{w}^{\mathrm{approx}}_{N_\theta,N} \right|_{L^\infty} \right\} / \left\{ \left| \tilde{w}^{\mathrm{ex}} \right|_{L^\infty} \right\}.$$

In a similar way, we passed $\{U^{\mathrm{ex}}, W^{\mathrm{ex}}\}$ to our HOPS algorithm to approximate IIOs giving, $\{\tilde{U}^{\mathrm{approx}}, \tilde{W}^{\mathrm{approx}}\}$, and computed the relative error

$$\mathrm{Error}_{\mathrm{rel}}^{\mathrm{IIO}} = \left\{ \left| \tilde{W}^{\mathrm{ex}} - \tilde{W}_{N_\theta,N}^{\mathrm{approx}} \right|_{L^\infty} \right\} / \left\{ \left| \tilde{W}^{\mathrm{ex}} \right|_{L^\infty} \right\}.$$

7.3. Robust Computation: DNOs versus IIOs. To begin we chose

$$\bar{g} = 0.5, \quad R^{(w)} = 0.3, \quad R^{(u)} = 0.8,$$

carried out the MMS simulations with our IIO method, (3.8), and report our results in Figures 2(a) and 2(b). We repeated this with our DNO approach [37] and display the outcomes in Figures 3(a) and 3(b). We see in this generic, non–resonant, configuration that both algorithms display a spectral rate of convergence as N is refined (up to the conditioning of the algorithm) which improves as ε is decreased.

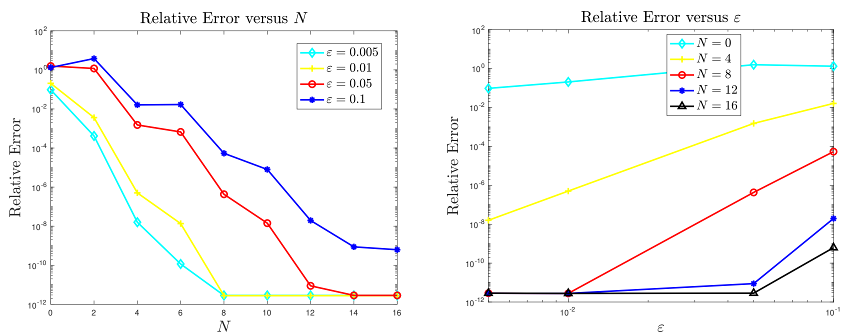

(a) Error in IIO formulation versus perturbation order, N.

(b) Error in IIO formulation versus perturbation size, ε.

FIG. 2. *Plot of relative error with five choices of* $N = 0, 4, 8, 12, 16$ *for a non–resonant configuration using the IIO formulation.*

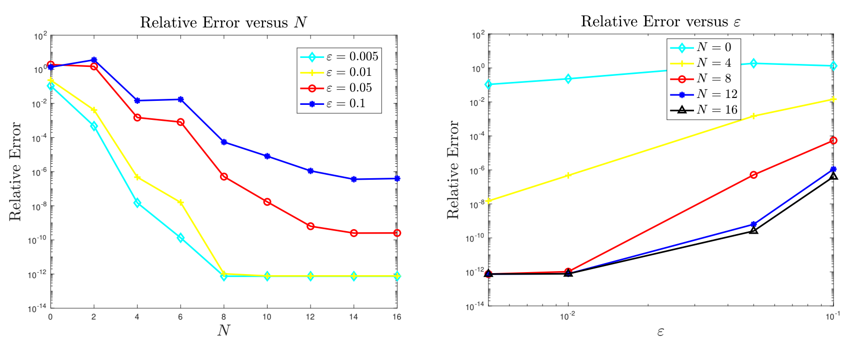

(a) Error in DNO formulation versus perturbation order, N.

(b) Error in DNO formulation versus perturbation size, ε.

FIG. 3. *Plot of relative error with five choices of* $N = 0, 4, 8, 12, 16$ *for a non–resonant configuration using the DNO formulation.*

Before proceeding, we note that the choice of radius $\bar{g} = 1$, will induce a singularity in the interior DNO resulting in a lack of uniqueness. To test performance of our methods near this scenario we selected

$$\bar{g} = 1 - \tau, \quad R^{(w)} = 0.6, \quad R^{(u)} = 1.6, \tag{7.4}$$

for two choices of τ. With the same choices of geometrical, (7.1), physical, (7.2), and numerical, (7.3), parameters as before, we selected $\tau = 10^{-12}$ resulting in $\bar{g} = 1 - 10^{-12}$. Once again, we conducted simulations with the IIO method, (3.8), and display our results in Figures 4(a) and 4(b). We revisited these computations with our DNO approach [37] and show our results in Figures 5(a) and 5(b). We see in this nearly resonant configuration, that while the IIO methodology continues to display a spectral rate of convergence as N is refined (improving as ε is decreased), the DNO approach does *not* provide results of the same quality.

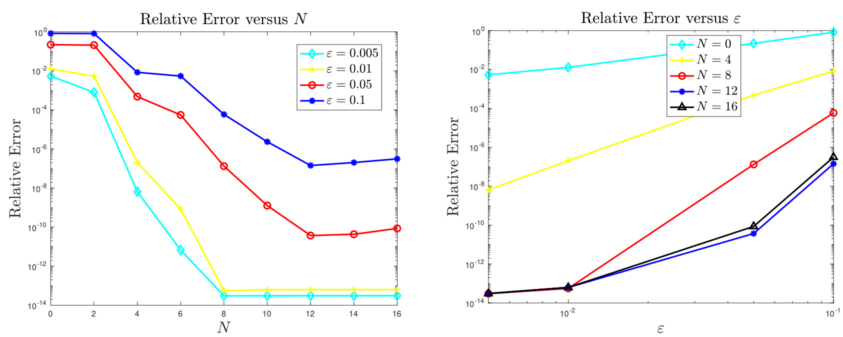

(a) Error in IIO formulation versus perturbation order, N.

(b) Error in IIO formulation versus perturbation size, ε.

FIG. 4. *Plot of relative error with five choices of* $N = 0, 4, 8, 12, 16$ *for a nearly resonant configuration using the IIO formulation.*

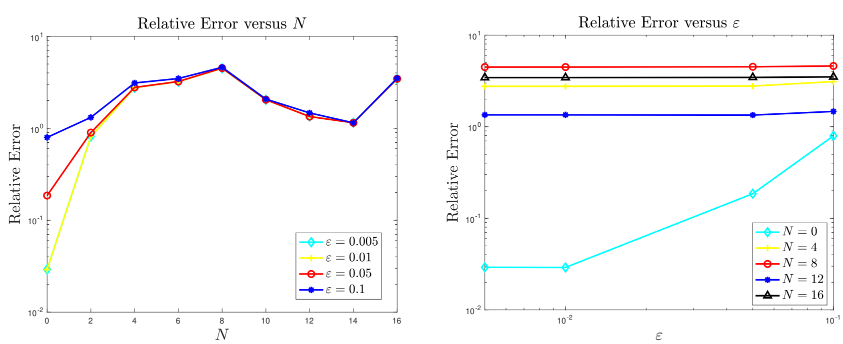

(a) Error in DNO formulation versus perturbation order, N.

(b) Error in DNO formulation versus perturbation size, ε.

FIG. 5. *Plot of relative error with five choices of* $N = 0, 4, 8, 12, 16$ *for a nearly resonant configuration using the DNO formulation.*

To close, we chose $\tau = 10^{-16}$ in (7.4) resulting in $\bar{g} = 1 - 10^{-16}$. After running simulations with the IIO method, (3.8), we display our results in Figures 6(a) and 6(b). We revisited these computations with our DNO approach [37] and show our results in Figures 7(a) and 7(b). We see in this resonant (to machine precision) configuration, the IIO again displays a spectral rate of convergence as N is refined (improving as ε is decreased), while the DNO approach delivers completely unacceptable results.

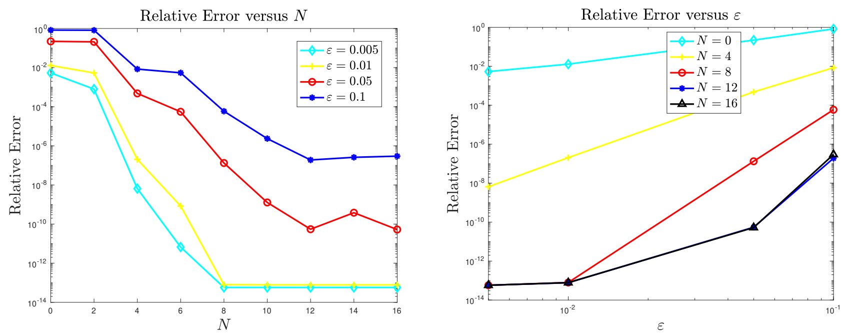

(a) Error in IIO formulation versus perturbation order, N.

(b) Error in IIO formulation versus perturbation size, ε.

FIG. 6. *Plot of relative error with five choices of* $N = 0, 4, 8, 12, 16$ *for a resonant configuration using the IIO formulation.*

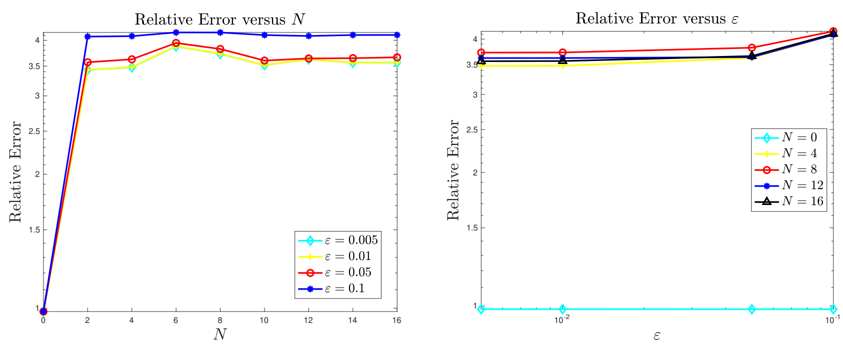

(a) Error in DNO formulation versus perturbation order, N.

(b) Error in DNO formulation versus perturbation size, ε.

FIG. 7. *Plot of relative error with five choices of* $N = 0, 4, 8, 12, 16$ *for a resonant configuration using the DNO formulation.*

7.4. Simulation of Nanorods. We close by returning to the problem of scattering of plane–wave incident radiation $u^{\text{inc}} = \exp(i\alpha x - i\gamma^u z)$ by a nanorod (which demands the Dirichlet and Neumann conditions, (2.1c) and (2.1d), respectively). More specifically, we considered metallic nanorods housed in a dielectric with outer interface shaped by $r = \bar{g} + g(\theta) = \bar{g} + \varepsilon f(\theta)$. We illuminated this structure over a range of incident wavelengths $\lambda_{\min} \le \lambda \le \lambda_{\max}$ and perturbation sizes $\varepsilon_{\min} \le \varepsilon \le \varepsilon_{\max}$, and computed the magnitudes of the reflected and transmitted surface currents, $\tilde{u}$ and $\tilde{w}$. These we term the “Reflection Map” and “Transmission Map” in analogy with similar quantities of interest in the study of metallic gratings [38, 23] Our study of the Fröhlich condition, (1.1), indicates that there should be a sizable enhancement in each at an LSPR. In the case of a nanorod with a perfectly circular cross–section we computed the value as the λ_F satisfying (1.1), and in subsequent plots this is depicted by a dashed red line.

Using the TFE approach to compute the IIOs, we studied the periodic sinusoidal profile

$$f(\theta) = \cos(4\theta), \tag{7.5}$$

see Figure 8. With this we considered the following physical configuration

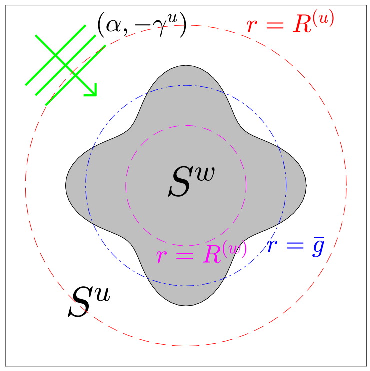

FIG. 8. *Plot of the cross–section of a metallic nanorod (occupying S^w) shaped by $r = \bar{g} + \varepsilon \cos(4\theta)$ ($\varepsilon = \bar{g}/5$) housed in a dielectric (occupying S^u) under plane–wave illumination with wavenumber $(\alpha, -\gamma^u)$. The dash–dot blue line depicts the unperturbed geometry, the circle $r = \bar{g}$.*

$$\begin{gathered}
\bar{g} = 0.025, \quad R^{(w)} = \bar{g}/10, \quad R^{(u)} = 10\bar{g}, \quad n^u = n^{\text{Vacuum}}, \quad n^w = n^{\text{Ag}}, \\
\lambda_{\text{min}} = 0.300, \quad \lambda_{\text{max}} = 0.800, \quad \varepsilon_{\text{min}} = 0, \quad \varepsilon_{\text{max}} = \bar{g}/5,
\end{gathered}$$

so that a silver (Ag) nanorod sits in vacuum, with numerical parameters

$$N_\lambda = 201, \quad N_\varepsilon = 201, \quad N_\theta = 32, \quad N_r = 16, \quad N = 8.$$

Plots of the Reflection Map and Transmission Map are displayed in Figure 9. In Figure 10 we show the final slice ($\varepsilon = \varepsilon_{\text{max}}$) of each of these, together with the Fröhlich value of the LSPR, (1.1), as a dashed red line. Here we see how even a

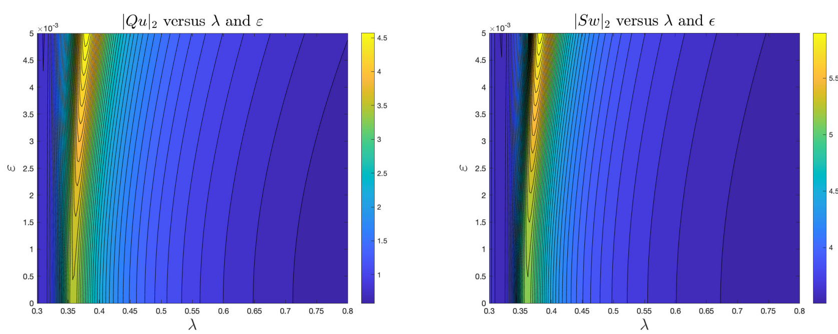

FIG. 9. *Reflection Map and Transmission Map for a silver nanorod shaped by the sinusoidal profile, (7.5), in vacuum. Here $\varepsilon_{max} = \bar{g}/5$, $\bar{g} = 0.025$, $\lambda_{min} = 0.300$, and $\lambda_{max} = 0.800$.*

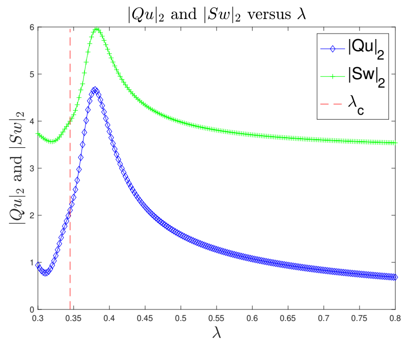

FIG. 10. *Final Slice of Reflection and Transmission Maps at $\varepsilon = \varepsilon_{max}$ for a silver nanorod shaped by the analytic profile,* (7.5)*, in vacuum.*

relatively moderate value of the deformation parameter (one fifth of the rod radius) can produce a sizable shift (about 40 nm from roughly 340 nm to 380 nm) in the LSPR location which our novel approach can accurately capture.

8. Conclusion. In this paper we have investigated a High–Order Perturbation of Surfaces (HOPS) algorithm for the numerical simulation of a novel formulation of the problem of scattering of linear waves by a nanorod in terms of Impedance–Impedance Operators (IIOs). Not only does our new methodology enjoy the same advantages of our previous implementation in terms of Dirichlet–Neumann Operators (e.g., surface formulation, exact enforcement of Sommerfeld radiation conditions, High–Order Spectral accuracy), but it is also immune to the Dirichlet eigenvalues which cause artificial singularities in our previous approach. In addition, our new formulation enables us to establish the existence, uniqueness, and analyticity of solutions to this problem, which we have taken pains to deliver. Finally, we have given a detailed description of our algorithm, and not only validated it but also demonstrated its efficiency, fidelity, and high–order accuracy.

The authors would like to thank P. Monk for an extensive correspondence on the conditions (3.2) and (3.3) which was very useful to the authors.

Appendix A. Existence, Uniqueness, and Regularity Theory.

In this appendix we state, and briefly prove, two existence, uniqueness, and regularity results for solutions of Helmholtz problems on simple interior and exterior domains.

A.1. The Exterior Problem. We begin by considering the Helmholtz problem posed on the *exterior* of a cylinder. For this we define

$$\Omega^{(u)} := \{\bar{g} < r < R^{(u)}\}, \quad \Gamma := \{r = \bar{g}\}, \quad \Sigma := \{r = R^{(u)}\},$$

where Σ is an artificial boundary. With these we can state our result.

THEOREM A.1. *Given an integer $s \geq 0$, if $F \in H^{s-1}(\Omega^{(u)})$, $U \in H^{s-1/2}(\Gamma)$, $K \in H^{s-1/2}(\Sigma)$, and Y is at most an order–one Fourier multiplier, there exists a* *unique solution of*

$$\Delta u + \epsilon^{(u)} k_0^2 u = F, \quad \textit{in } \Omega^{(u)}, \tag{A.1a}$$

$$-\tau^u \partial_r u + Y u = U, \quad \textit{at } \Gamma, \tag{A.1b}$$

$$\partial_r u + T^{(u)}[u] = K, \quad \textit{at } \Sigma. \tag{A.1c}$$

where $\epsilon^{(u)} \in \mathbf{R}^+$*, satisfying*

$$\|u\|_{H^{s+1}} \leq C_e^{(u)} \left\{ \|F\|_{H^{s-1}} + \|U\|_{H^{s-1/2}} + \|K\|_{H^{s-1/2}} \right\}, \tag{A.2}$$

where $C_e^{(u)} > 0$ *is a universal constant, provided that*

$$\operatorname{Im}\left\{ \int_\Gamma \left(\left(\frac{Y}{\tau^u} \right) u \right) \overline{u}\, ds \right\} \leq 0. \tag{A.3}$$

Proof. Following [15, 7, 30] we consider the weak formulation

$$\mathcal{A}^{(u)}(u,\phi) + \mathcal{D}^{(u)}(u,\phi) + \mathcal{E}^{(u)}(u,\phi) = \mathcal{L}^{(u)}(\phi),$$

where

$$\begin{aligned}
\mathcal{A}^{(u)}(u,\phi) &:= \int_{\Omega^{(u)}} \nabla u \cdot \overline{\nabla \phi} + u\overline{\phi}\, dV \\
&\qquad - \operatorname{Re}\left\{ \int_\Sigma (\partial_r u)\overline{\phi}\, ds \right\} + \operatorname{Re}\left\{ \int_\Gamma \left(\left(\frac{Y}{\tau^u} \right) u \right) \overline{\phi}\, ds \right\}, \\
\mathcal{D}^{(u)}(u,\phi) &:= -\left(\epsilon^{(u)} k_0^2 + 1 \right) \int_{\Omega^{(u)}} u\overline{\phi}\, dV, \\
\mathcal{E}^{(u)}(u,\phi) &:= -\operatorname{Im}\left\{ \int_\Sigma (\partial_r u)\overline{\phi}\, ds \right\} + \operatorname{Im}\left\{ \int_\Gamma \left(\left(\frac{Y}{\tau^u} \right) u \right) \overline{\phi}\, ds \right\}, \\
\mathcal{L}^{(u)}(\phi) &:= -\int_{\Omega^{(u)}} F\overline{\phi}\, dV + \int_\Sigma K\overline{\phi}\, ds - \int_\Gamma \left(\frac{U}{\tau^u} \right) \overline{\phi}\, ds.
\end{aligned}$$

In order to resolve the *uniqueness* of solutions, we study this formulation when $F \equiv U \equiv K \equiv 0$ and prove that $u \equiv 0$. For this we choose $\phi = u$ and recall that $\epsilon^{(u)} \in \mathbf{R}$, so that it is clear that the imaginary part of the weak formulation is simply $\mathcal{E}^{(u)}$. Enforcing that this be zero demands

$$\operatorname{Im}\left\{ \int_\Sigma (\partial_r u)\overline{u}\, ds \right\} = \operatorname{Im}\left\{ \int_\Gamma \left(\left(\frac{Y}{\tau^u} \right) u \right) \overline{u}\, ds \right\}.$$

Rellich's Lemma [6] tells us that $u \equiv 0$ provided that

$$\int_\Sigma (\partial_r u)\overline{u}\, ds \leq 0, \quad R^{(u)} \to \infty,$$

so that a condition for uniqueness of solutions is (A.3).

Regarding existence of solutions and the estimate (A.2), we follow [15, 7, 30] and note that, for $V = H^1(\Omega^{(u)})$, $\mathcal{A}^{(u)}$ is a continuous, sesquilinear form from $V \times V$ to $\mathbf{C}$ which induces a bounded operator $\mathbf{A} : V \to V'$ (see Lemma 2.1.38 of [41]). While the first two terms are standard the fourth requires that Y be at most a bounded, order–one Fourier multiplier. The third can be addressed by noting that

$$\int_\Sigma (\partial_r u)\overline{\phi}\, ds = \int_\Sigma \left(-T^{(u)} u \right) \bar{\phi}\, ds,$$

c.f., (2.3b), and using the fact that $T^{(u)}$ is an order–one Fourier multiplier [15, 7, 30].

Furthermore, $\mathcal{A}$ is V–elliptic [41], i.e., there is a $\gamma > 0$ such that

$$\mathrm{Re}\left\{\mathcal{A}(v, v)\right\} \leq \gamma \left\|v\right\|_V^2 .$$

The first two terms are the V–norm causing no problem. The second two terms require

$$\mathrm{Re}\left\{\int_\Gamma \left(\left(\frac{Y}{\tau}\right) u\right) \bar{u}\, ds\right\} \geq 0, \quad \mathrm{Re}\left\{\int_\Sigma \left(-T^{(u)} u\right) \bar{u}\, ds\right\} \leq 0.$$

However, as $T^{(u)} = -H_p'(k^u R^{(u)})/H_p(k^u R^{(u)})$ and Shen and Wang [42] have shown that

$$\mathrm{Re}\left\{-T^{(u)}\right\} \leq 0,$$

we have the V–ellipticity of $\mathcal{A}$. By the Lax–Milgram Lemma (see Lemma 2.1.51 of [41]) the operator $\mathbf{A}$ satisfies

$$\left\|\mathbf{A}^{-1}\right\|_{V \leftarrow V'} \leq \frac{1}{\gamma}.$$

It is not difficult to show that $\mathcal{D}$ and $\mathcal{E}$ induce bounded operators $\mathbf{D}$ and $\mathbf{E}$ from $L^2(\Omega^{(u)})$ to $L^2(\Omega^{(u)})$ which are compact as V embeds compactly into $L^2(\Omega^{(u)})$ [41]. Fredholm's theory [15, 7, 30] delivers a solution with the appropriate estimates provided that the solution is unique (which we have just established). □

A.2. The Interior Problem. The other Helmholtz problem which arises in our developments is stated on the *interior* of a cylinder. Here we denote

$$\Omega^{(w)} := \{r < \bar{g}\}, \quad \Gamma := \{r = \bar{g}\},$$

and we can now state our result.

THEOREM A.2. *Given an integer $s \geq 0$, if $F \in H^{s-1}(\Omega^{(w)})$ $W \in H^{s-1/2}(\Gamma)$, Z is at most an order–one Fourier multiplier, there exists a unique bounded solution of*

$$\Delta w + \epsilon^{(w)} k_0^2 w = F, \quad \textit{in } \Omega^{(w)}, \tag{A.4a}$$

$$\tau^w \partial_r w - Z w = W, \quad \textit{at } \Gamma. \tag{A.4b}$$

where $\mathrm{Im}\left\{\epsilon^{(w)}\right\} \geq 0$, *satisfying*

$$\left\|w\right\|_{H^{s+1}} \leq C_e^{(w)} \left\{\left\|F\right\|_{H^{s-1}} + \left\|W\right\|_{H^{s-1/2}}\right\}, \tag{A.5}$$

where $C_e^{(w)} > 0$ is a universal constant, provided that

$$\mathrm{Im}\left\{\int_\Gamma \left(\left(\frac{Z}{\tau^w}\right) w\right) \overline{w}\, ds\right\} \geq 0. \tag{A.6}$$

Proof. As before, we imitate [15, 7, 30] and study the following weak formulation

$$\mathcal{A}^{(w)}(w, \phi) + \mathcal{D}_1^{(w)}(w, \phi) + \mathcal{D}_2^{(w)}(w, \phi) + \mathcal{E}^{(w)}(w, \phi) = \mathcal{L}^{(w)}(\phi),$$

where,

$$\mathcal{A}^{(w)}(w,\phi) := \int_{\Omega^{(w)}} \nabla w \cdot \overline{\nabla \phi} + w\overline{\phi}\, dV - \mathrm{Re}\left\{ \int_{\Gamma_g} \left(\left(\frac{Z}{\tau} \right) w \right) \overline{\phi}\, ds \right\},$$

$$\mathcal{D}_1^{(w)}(w,\phi) := -\left(\mathrm{Re}\left\{ \epsilon^{(w)} \right\} k_0^2 + 1 \right) \int_{\Omega^{(w)}} w\overline{\phi}\, dV,$$

$$\mathcal{D}_2^{(w)}(w,\phi) := -\left(\mathrm{Im}\left\{ \epsilon^{(w)} \right\} k_0^2 \right) \int_{\Omega^{(w)}} w\overline{\phi}\, dV,$$

$$\mathcal{E}^{(w)}(w,\phi) := -\mathrm{Im}\left\{ \int_{\Gamma_g} \left(\left(\frac{Z}{\tau^w} \right) w \right) \overline{\phi}\, ds \right\},$$

$$\mathcal{L}^{(w)}(\phi) := \int_{\Omega^{(w)}} G\overline{\phi}\, dV + \int_{\Gamma} \frac{W}{\tau^w} \overline{\phi}\, ds.$$

As before, to study *uniqueness* we consider $G \equiv W \equiv 0$ and establish that $w \equiv 0$. If we choose $\phi = w$ then it is clear that the imaginary part of the weak formulation is simply portions of $\mathcal{D}_2^{(w)} + \mathcal{E}^{(w)}$ and enforcing that this be zero demands

$$\left(\mathrm{Im}\left\{ \epsilon^{(w)} \right\} k_0^2 \right) \int_{\Omega^{(w)}} |w|^2 \; dV = -\int_{\Gamma} \left(\left(\mathrm{Im}\left\{ \frac{1}{\tau^w} \right\} Z \right) w \right) \overline{w}\, ds.$$

If we consider $\mathrm{Im}\left\{ \epsilon^{(w)} \right\} \geq 0$, then $\int_{\Omega^{(w)}} |w|^2 \; dV \leq 0$, implies $w \equiv 0$ if (A.6) is verified.

The existence of solutions and the estimate (A.5) are proven in analogous fashion to Theorem A.1 and we leave the details to the motivated reader. $\square$

REFERENCES

[1] H. Ammari, P. Millien, M. Ruiz, and H. Zhang, *Mathematical analysis of plasmonic nanoparticles: the scalar case*, Arch. Ration. Mech. Anal., 224 (2017), pp. 597–658.
[2] G. A. Baker, Jr. and P. Graves-Morris, *Padé approximants*, Cambridge University Press, Cambridge, second ed., 1996.
[3] A.-S. Bonnet-Ben Dhia, C. Carvalho, L. Chesnel, and P. Ciarlet, Jr., *On the use of perfectly matched layers at corners for scattering problems with sign-changing coefficients*, J. Comput. Phys., 322 (2016), pp. 224–247.
[4] O. Bruno and F. Reitich, *Numerical solution of diffraction problems: A method of variation of boundaries. II. Finitely conducting gratings, Padé approximants, and singularities*, J. Opt. Soc. Am. A, 10 (1993), pp. 2307–2316.
[5] O. R. Burggraf, *Analytical and numerical studies of the structure of steady separated flows*, J. Fluid Mech., 24 (1966), pp. 113–151.
[6] D. Colton and R. Kress, *Inverse acoustic and electromagnetic scattering theory*, vol. 93 of Applied Mathematical Sciences, Springer, New York, third ed., 2013.
[7] L. Demkowicz and F. Ihlenburg, *Analysis of a coupled finite-infinite element method for exterior Helmholtz problems*, Numer. Math., 88 (2001), pp. 43–73.
[8] B. Després, *Domain decomposition method and the Helmholtz problem*, in Mathematical and numerical aspects of wave propagation phenomena (Strasbourg, 1991), SIAM, Philadelphia, PA, 1991, pp. 44–52.
[9] M. O. Deville, P. F. Fischer, and E. H. Mund, *High-order methods for incompressible fluid flow*, vol. 9 of Cambridge Monographs on Applied and Computational Mathematics, Cambridge University Press, Cambridge, 2002.
[10] I. El-Sayed, X. Huang, and M. El-Sayed, *Selective laser photo-thermal therapy of epithelial carcinoma using anti-egfr antibody conjugated gold nanoparticles*, Cancer Lett., 239 (2006), pp. 129–135.
[11] L. C. Evans, *Partial differential equations*, American Mathematical Society, Providence, RI, second ed., 2010.

[12] G. B. Folland, *Introduction to partial differential equations*, Princeton University Press, Princeton, N.J., 1976. Preliminary informal notes of university courses and seminars in mathematics, Mathematical Notes.
[13] D. Gottlieb and S. A. Orszag, *Numerical analysis of spectral methods: theory and applications*, Society for Industrial and Applied Mathematics, Philadelphia, Pa., 1977. CBMS-NSF Regional Conference Series in Applied Mathematics, No. 26.
[14] L. Greengard and V. Rokhlin, *A fast algorithm for particle simulations*, J. Comput. Phys., 73 (1987), pp. 325–348.
[15] I. Harari and T. J. R. Hughes, *Analysis of continuous formulations underlying the computation of time-harmonic acoustics in exterior domains*, Comput. Methods Appl. Mech. Engrg., 97 (1992), pp. 103–124.
[16] J. Helsing and A. Karlsson, *On a Helmholtz transmission problem in planar domains with corners*, J. Comput. Phys., 371 (2018), pp. 315–332.
[17] J. S. Hesthaven and T. Warburton, *Nodal discontinuous Galerkin methods*, vol. 54 of Texts in Applied Mathematics, Springer, New York, 2008. Algorithms, analysis, and applications.
[18] C. Johnson, *Numerical solution of partial differential equations by the finite element method*, Cambridge University Press, Cambridge, 1987.
[19] R. Kress, *Linear integral equations*, Springer-Verlag, New York, third ed., 2014.
[20] J. Lai and M. O'Neil, *An FFT-accelerated direct solver for electromagnetic scattering from penetrable axisymmetric objects*, J. Comput. Phys., 390 (2019), pp. 152–174.
[21] R. J. LeVeque, *Finite difference methods for ordinary and partial differential equations*, Society for Industrial and Applied Mathematics (SIAM), Philadelphia, PA, 2007. Steady-state and time-dependent problems.
[22] C. Loo, A. Lowery, N. Halas, J. West, and R. Drezek, *Immunotargeted nanoshells for integrated cancer imaging and therapy*, Nano Letters, 5 (2005), pp. 709–711.
[23] S. A. Maier, *Plasmonics: Fundamentals and Applications*, Springer, New York, 2007.
[24] A. Moiola and E. A. Spence, *Acoustic transmission problems: wavenumber-explicit bounds and resonance-free regions*, Math. Models Methods Appl. Sci., 29 (2019), pp. 317–354.
[25] V. Myroshnychenko, E. Carbo-Argibay, I. Pastoriza-Santos, J. Perez-Juste, L. Liz-Marzan, and F. Garcia de Abajo, *Modeling the optical response of highly faceted metal nanoparticles with a fully 3d boundary element method*, Advanced Materials, 20 (2008), pp. 4288–4293.
[26] V. Myroshnychenko, J. Rodriguez-Fernandez, I. Pastoriza-Santos, A. Funston, C. Novo, P. Mulvaney, L. Liz-Marzan, and J. Garcia de Abajo, *Modelling the optical response of gold nanoparticles*, Chemical Society Reviews, 37 (2008), pp. 1792–1805.
[27] D. P. Nicholls, *Three–dimensional acoustic scattering by layered media: A novel surface formulation with operator expansions implementation*, Proceedings of the Royal Society of London, A, 468 (2012), pp. 731–758.
[28] D. P. Nicholls, *On analyticity of linear waves scattered by a layered medium*, Journal of Differential Equations, 263 (2017), pp. 5042–5089.
[29] D. P. Nicholls and N. Nigam, *Exact non-reflecting boundary conditions on general domains*, J. Comput. Phys., 194 (2004), pp. 278–303.
[30] D. P. Nicholls and N. Nigam, *Error analysis of an enhanced DtN–fe method for exterior scattering problems*, Numer. Math., 105 (2006), pp. 267–298.
[31] D. P. Nicholls and F. Reitich, *A new approach to analyticity of Dirichlet-Neumann operators*, Proc. Roy. Soc. Edinburgh Sect. A, 131 (2001), pp. 1411–1433.
[32] D. P. Nicholls and F. Reitich, *Stability of high-order perturbative methods for the computation of Dirichlet-Neumann operators*, J. Comput. Phys., 170 (2001), pp. 276–298.
[33] D. P. Nicholls and F. Reitich, *Analytic continuation of Dirichlet-Neumann operators*, Numer. Math., 94 (2003), pp. 107–146.
[34] D. P. Nicholls and F. Reitich, *Shape deformations in rough surface scattering: Improved algorithms*, J. Opt. Soc. Am. A, 21 (2004), pp. 606–621.
[35] D. P. Nicholls and J. Shen, *A stable, high–order method for two–dimensional bounded–obstacle scattering*, SIAM J. Sci. Comput., 28 (2006), pp. 1398–1419.
[36] D. P. Nicholls and J. Shen, *A rigorous numerical analysis of the transformed field expansion method*, SIAM Journal on Numerical Analysis, 47 (2009), pp. 2708–2734.
[37] D. P. Nicholls and X. Tong, *A high–order perturbation of surfaces algorithm for the simulation of localized surface plasmon resonances in two dimensions*, J. Sci. Comput., 76 (2018), pp. 1370–1395.
[38] H. Raether, *Surface plasmons on smooth and rough surfaces and on gratings*, Springer, Berlin, 1988.
[39] L. Rayleigh, *On the dynamical theory of gratings*, Proc. Roy. Soc. London, A79 (1907),

pp. 399–416.
[40] S. O. Rice, *Reflection of electromagnetic waves from slightly rough surfaces*, Comm. Pure Appl. Math., 4 (1951), pp. 351–378.
[41] S. A. Sauter and C. Schwab, *Boundary element methods*, vol. 39 of Springer Series in Computational Mathematics, Springer-Verlag, Berlin, 2011. Translated and expanded from the 2004 German original.
[42] J. Shen and L.-L. Wang, *Analysis of a spectral-Galerkin approximation to the Helmholtz equation in exterior domains*, SIAM J. Numer. Anal., 45 (2007), pp. 1954–1978.
[43] H. Xu, E. Bjerneld, M. Käll, and L. Börjesson, *Spectroscopy of single hemoglobin molecules by surface enhanced raman scattering*, Phys. Rev. Lett., 83 (1999), pp. 4357–4360.